SUPPORTING ONLINE MATERIAL FOR RASER AND O'SHEA

Materials and methods

YEAST STRAINS AND MEDIA

The coding sequence for yeast-optimized enhanced cyan fluorescent protein (yECFP) was constructed by incorporation of the following mutations into the yEGFP1 sequence (*S1*): Y66W, N146I, M153T, V163A, S175G (*S2-S4*). Yeast-optimized Venus yellow fluorescent protein (yVYFP) was constructed by incorporation of the following mutations into the yEGFP3 sequence (*S1*): F46L, F64L, V68L, Q69M, M153T, V163A, S175G, T203Y (*S5, S6*). The excitation and emission spectra were verified by fluorimetry of bacterial lysates expressing the yECFP and yVYFP proteins. A yeast chromosomal integration vector, pJRL2, that replaces the *LEU2* chromosomal locus by homologous recombination, was constructed by insertion of the 200 bp upstream of the *LEU2* start codon, an Asc I restriction enzyme site, the 200 bp downstream of the *LEU2* stop codon and a 5.5 kb *hisG::URA3::kanR::hisG* cassette (*S7*) into pBluescript (Stratagene).

All constructs for dual-reporter noise measurements contained 1000 bp of promoter sequence, from the nucleotide immediately upstream of the relevant start codon, followed by six base-pairs of idealized Kozak sequence AACAAA for optimal translational initiation (*S8*), the coding sequence of the appropriate fluorophore (yECFP or yVYFP) and the 500 bp 3' to the stop codon of *ACT1* in the pJRL2 integrating vector. Constructs expressing YFP were integrated into W303-derivative EY1555 (*MAT***a** *trp1 HIS3 ADE2*), constructs expressing CFP were integrated into W303-derivative EY1556 (*MATα TRP1 his3 ADE2)*, and diploids were obtained by mating and double selection.

PHO5 promoter variants were constructed by PCR using primers containing the desired mutations. UASm1 and UASm2 mutants have been previously described (*S9*). The TATA variant nomenclature indicates the mutation introduced into the wild-type PHO5 TATA box, e.g. TATA-A1 converts TATATAAG to AATATAAG. *PHO5-GAL1* and *GAL1-PHO5* fusions were constructed by PCR using primers containing the desired junction sequences (for *GAL1-PHO5*, the *PHO5* promoter sequence from -83 to the -1 position relative to the *PHO5* ATG was fused to the upstream portion of the *GAL1* promoter after the -129 position relative to the *GAL1* ATG; for *PHO5-GAL1*, the *GAL1* promoter sequence from -128 to the -1 position relative to the *GAL1* ATG was fused to the upstream portion of the *PHO5* promoter after the -84 position relative to the *PHO5* ATG; both fusions preserve the native promoter TATA box). The yeast deletion strains were made as described previously (*S9*) from strains containing integrated *PHO5prCFP* and *PHO5prYFP*. The chemical inhibitor-sensitive ($PHO85^{F82G}$) strains containing *PHO5prCFP* and *PHO5prYFP* were constructed as described previously (*S9*).

Unless otherwise indicated, yeast strains were grown at 30°C in synthetic complete medium containing glucose with addition of 0.1 mg/mL adenine and 0.1 mg/mL tryptophan to suppress autofluorescence. The *PHO84* promoter was induced with synthetic phosphate-free medium containing levels of inorganic phosphate ranging from 0 to 500 micromolar (*S10*). The *GAL1* promoter was induced with medium containing 2% raffinose and levels of galactose from 0 to 2%. The *PHO5* promoter was induced either in medium containing levels from 0 to 10 micromolar of a chemical inhibitor (1-NaPP1) of a specific allele of *PHO85* (*S11*); or in synthetic phosphate-free

medium containing levels of phytic acid from 0 to 600 micromolar as an organic phosphate source.

NOISE MEASUREMENTS

For noise measurement time-courses, cells were grown overnight in 50 mL batch cultures to an OD_{600} of less than 0.4, rapidly washed in water, and transferred to 200 mL of the appropriate induction medium. Subpopulations (~20 mL) were harvested at different time points, placed on ice, sonicated, and concentrated in order to prepare for microscopy. The chilled, sonicated cells were imaged on glass slides in standard medium.

Microscopy was conducted using a digital imaging-capable Nikon TE200/300 inverted microscope with an oil-immersed objective at X 60 magnification. Using a script in MetaMorph version 4.6r8 imaging software (Universal Imaging Corporation), Nomarski/DIC (differential interference constrast) and YFP, CFP, and RFP fluorescence images were taken in rapid succession. For each population, images of 12 fields containing 80-150 cells were obtained. MetaMorph was used for image analysis, which included background subtraction, elimination of dead or CFP-autofluorescent cells by RFP channel fluorescence (~5% of cells), and quantitation of CFP and YFP values for each individual cell. The CFP population mean value was scaled to the YFP population mean for each independent population of cells, and a maximal induction control was performed in parallel for each experiment in order to account for daily variation in fluorescence intensity measurements (though such variation was minimal). For low level inductions of the *GAL1* promoter, bimodal populations were scaled individually. Less than 0.1% of all cells clearly expressed only one of the two fluorophores, and were

eliminated from analysis. Rates of expression were calculated from linear fits of the increase in mean population fluorescence over time. All average noise strength values presented are the average of values from a single induction time course. All experiments were repeated at least three times and resulted in the same trends each time. Bootstrap values (90%) for Fig. 1C were calculated by random selection of populations of the same size as the original populations. Error bars for Figs. 2 and 4 represent standard deviations. Flow cytometry fluorescence measurements and sorting by forward scatter and side scatter (<5% of total population) were performed using a FACSAria (BD Biosciences). For flow cytometry sorting experiments, cells were sorted and then processed for fluorescence microscopy as described above. Cellular volume was estimated by measurement of the area of each cell from DIC images. A simple budding index, in which cells that were unbudded or had small buds were scored as "G1" and cells with large buds were scored as "S/G2/M" based on DIC images, was used to stratify by cell cycle stage.

For the measurement of correlation of expression between two different promoters, expression from the promoters was induced by growth for 6 hours in synthetic phosphate-free medium containing 2% dextrose for the *PHO84/ADH1* measurements, and by synthetic phosphate-free medium containing 2% galactose for the *PHO84/GAL1* measurements.

STOCHASTIC SIMULATIONS

Efficient exact stochastic simulations were performed according to the Next Reaction Method (*S12, S13*) and implemented in MatLab (The MathWorks). The base constants chosen for the simulations were as follows in the form $\{k_a\ k_m\ k_p\ \gamma_a\ \gamma_m\ \gamma_p\}$: case

I, {0.1 10 10 0.1 5 0.1}; case II, {0.53 100 10 10 5 0.1}; case III, {53 100 10 1000 5 0.1}. The forward rates of promoter activation, transcription, and translation were varied individually as necessary to produce a range of steady-state protein levels. Induction time course simulations were analyzed at t = 100, 200, 300 for cases I and II, and t = 10, 20, 30 for case III with independent populations of 100 simulated cells with a single gene. No extrinsic noise factors were included in the simulation, and therefore the intrinsic noise strength was calculated from the total noise strength.

Fluorescent reporter equivalence and independence

The separation of noise into extrinsic and intrinsic components by a dual-reporter technique requires that the reporters be both equivalent and independent (*S14, S15*). To be equivalent, reporters must have similar kinetics for all the reactions of gene expression. Independence requires that the presence of one reporter gene or protein product does not affect expression or measurement of the other reporter gene. *A priori*, cyan fluorescent protein and yellow fluorescent protein should satisfy the requirement of equivalence, as they represent allelic variants of the green fluorescent protein, and are therefore nearly identical in sequence. Also, the yeast-optimized variants used in this study were constructed to be as similar as possible in terms of stability and thermosensitivity (see materials and methods). In order to be independent, the reporter genes, mRNAs and proteins must not selectively saturate factors required for gene expression (*S15*). We expect that the promoter-specific transcriptional activators and general transcriptional and translational machinery are not limiting; we also assume that the fluorescent protein products are not capable of feedback regulation of their own

transcription or translation. Also, we assume that the two identical promoters do not display coordinate regulation *in trans*; such regulation would cause underestimation of the stochastic contribution to population variability by our measurement technique.

To test these assumptions of equivalence and independence, we constructed yeast strains containing each single reporter under the control of the *PHO5* promoter, and measured the population mean and noise for four time points from an induction time course in response to phosphate starvation. The strain expressing only CFP displayed CFP fluorescence distributions indistinguishable from those of the CFP/YFP strain at each time point (P = 0.71, 0.54, 0.78, 0.97 by Kolmogorov-Smirnov tests). The strain expressing only YFP displayed YFP fluorescence distributions indistinguishable from those of the CFP/YFP strain at each time point (P = 0.27, 0.56, 0.43, 0.44 by Kolmogorov-Smirnov tests). In the strain expressing both reporters, the CFP and YFP fluorescence distributions were indistinguishable for each time point (P = 0.74, 0.82, 1.00, 0.99 by Kolmogorov-Smirnov tests). In addition, we used the single-fluorophore measurements to confirm that YFP and CFP fluorescence are fully separable in our measurement system; the contribution of YFP fluorescence to measured CFP fluorescence is <0.1% and the contribution of CFP fluorescence to measured YFP fluorescence is <0.2%.

Definition of intrinsic, extrinsic, and total noise and noise strength

In the following description, we adhere to the basic definitions of the noise η as $\sigma_p/\langle p\rangle$, or the standard deviation of the protein number per cell divided by the mean protein number. Normalized variance η^2 is defined as $\sigma_p^2/\langle p\rangle^2$ and the Fano factor or

noise strength ν is $\sigma_p^2/\langle p \rangle$. Elowitz et al. and Swain et al. defined the total, intrinsic, and extrinsic normalized variance in their dual independent reporter system in the following manner (*S14, S16*):

$$\begin{aligned} \eta^2_{\text{total}} &= \eta^2_{\text{intrinsic}} + \eta^2_{\text{extrinsic}} \\ \eta^2_{\text{intrinsic}} &= \frac{\langle (c-y)^2 \rangle}{2\langle c \rangle \langle y \rangle} \\ \eta^2_{\text{extrinsic}} &= \frac{\langle cy \rangle - \langle c \rangle \langle y \rangle}{\langle c \rangle \langle y \rangle} \end{aligned} \qquad \textbf{[1]}$$

where c and y represent CFP and YFP fluorescence per cell, respectively.

The corresponding noise strength ν can be calculated by multiplication of the normalized variance η^2 by the mean:

$$\begin{aligned} \nu_{\text{total}} &= \eta^2_{\text{total}} \sqrt{\langle c \rangle \langle y \rangle} \\ \nu_{\text{intrinsic}} &= \frac{\langle (c-y)^2 \rangle}{2\sqrt{\langle c \rangle \langle y \rangle}} \\ \nu_{\text{extrinsic}} &= \frac{\langle cy \rangle - \langle c \rangle \langle y \rangle}{\sqrt{\langle c \rangle \langle y \rangle}} \end{aligned} \qquad \textbf{[2]}$$

As the intrinsic and extrinsic components of the normalized variance are directly additive, the intrinsic and extrinsic noise strength are additive as well.

Intrinsic error of measurement

A component of the intrinsic noise or intrinsic noise strength will be due to systematic errors of measurement in our system. To estimate the magnitude of the intrinsic error of measurement, we constructed a yeast strain expressing green fluorescent protein (GFP) from the *MET3* promoter, induced expression of GFP by methionine starvation, and measured the GFP fluorescence per cell using the YFP excitation/emission filter set, and using the CFP excitation/YFP emission filters. We then

calculated intrinsic noise and intrinsic noise strength for these cell populations as if the YFP and CFP/YFP measurements were independent fluorophores. The intrinsic noise strength was <0.25 AU in all cases, and was mainly attributable to yeast autofluorescence in the CFP excitation/YFP emission measurement. During the actual measurements of strains containing CFP and YFP, autofluorescence in the CFP excitation/CFP emission filter set was significantly smaller than the autofluorescence of this control (data not shown), so we suspect this intrinsic error of measurement is an overestimate of the error in our measurement system.

Measured intrinsic noise is consistent with a stochastic process

For the *PHO5* promoter, the intrinsic noise decreases from 45% to 5% over the induction time course shown in Fig. 1B (Fig. S4A). In contrast to the extrinsic or total noise, the intrinsic noise decreases in proportion to the inverse square-root of the mean of gene expression, consistent with a single underlying stochastic process. This relationship is equivalent to both a linear relationship between the inverse mean and the normalized variance (Fig. S4B) and the constant relationship seen between population mean and the intrinsic noise strength (Fig. 1C).

The intrinsic noise measured in our experiments could result from ongoing stochastic events in gene expression or from a stochastic delay between activation of the two alleles followed by deterministic gene expression. The delay model predicts that the maximal and average difference between CFP and YFP per cell in a population of cells during induction will decrease over time and reach zero at steady-state levels of induction. We measured the intrinsic noise of the constitutively active promoter *ADH1* at

steady-state and find that the intrinsic noise strength is >4-fold over the limit of detection. Additionally, during induction time courses of the *PHO5* promoter, the maximal and average difference between CFP and YFP per cell increases after >90% of the cells have induced both alleles for 7 of 7 time courses examined. For example, for the six time points of the induction time course shown in Fig. 1B, the average differences between CFP and YFP per cell are 5, 16, 18, 23, 21, and 21 AU for the 60', 90', 135', 180', 270' and 360' populations, and the maximal differences between CFP and YFP for any one cell are 27, 45, 75, 84, 73, and 98 AU, respectively. 100% of the cells have induced both CFP and YFP expression by the second time point (90') in this series.

Both the observation of intrinsic noise at steady-state for *ADH1*, and the increase in the difference between CFP and YFP after both alleles have induced *PHO5*, support a model in which intrinsic noise is not solely a consequence of an initial difference in the timing of induction of each allele followed by deterministic gene expression. We conclude that the intrinsic noise in our measurement system is attributable to stochasticity in gene expression, and that stochastic events are not limited to the initial induction period but occur during active gene expression.

Comparison with a previous study of noise of the *GAL1* promoter

A previous study measured noise strength in gene expression in *S. cerevisiae* with a single fluorescent reporter (*S17*). This study examined the noise of a modified version of the *GAL1* promoter. Our observations for *GAL1* differ from the conclusions of this study which reported a profile of noise strength as a function of transcription rate qualitatively similar to that which we observe for the extrinsic and total noise strength

(Fig. S1). This discrepancy may result from differences in strains or experimental details, or may reflect the fact that the technique used previously was unable to discriminate between intrinsic and extrinsic noise sources.

Solution of the master equation for steady-state normalized variance

Construction and steady-state solution of the moment generating function for the master equation for the model shown in figure 3A was undertaken as previously described (*S18*). The resulting steady-state noise equation, expressed in the form of normalized variance, must conform to the general equation described previously (*S15*):

$$\eta^2_{\text{int}} = \underbrace{\frac{\sigma^2_p}{\langle p\rangle^2}}_{\text{protein}} + \underbrace{\frac{\sigma^2_m}{\langle m\rangle^2}\cdot t_{m\to p}}_{\text{mRNA}} + \underbrace{\frac{\sigma^2_a}{\langle a\rangle^2}\cdot t_{a\to p}}_{\text{active gene}} \qquad \textbf{[3]}$$

where the *t* represents the time-averaging contributions, *p* refers to protein, *m* to mRNA, *a* to the active gene, and the normalized variance terms refer to each molecular species in isolation. These terms are part of the intrinsic noise definition of the dual-reporter system; any noise terms due to signaling upstream of the promoter or constant noise contributions due to population heterogeneity are part of the extrinsic noise definition and therefore do not appear in this expression.

We note that the binomial distribution applies to the active DNA species, and set the gene number to one. We incorporate the results from the calculation of variance from differentiation of the master equation moment generating function (*S18*) and rewrite the normalized variance expression as noise strength by multiplication by the protein mean.

$$\nu_{\text{int}} = 1 + \mathrm{E}_{m\to p}\cdot\frac{\gamma_{\mathrm{m}}}{\gamma_{\mathrm{m}}+\gamma_{\mathrm{p}}} + \mathrm{E}_{m\to p}\mathrm{E}_{a\to m}\cdot\frac{(1-\langle a\rangle)(\mathrm{k}_{\mathrm{a}}+\gamma_{\mathrm{a}}+\gamma_{\mathrm{m}}+\gamma_{\mathrm{p}})\gamma_{\mathrm{a}}\gamma_{\mathrm{m}}}{(\mathrm{k}_{\mathrm{a}}+\gamma_{\mathrm{a}}+\gamma_{\mathrm{m}})(\gamma_{\mathrm{m}}+\gamma_{\mathrm{p}})(\mathrm{k}_{\mathrm{a}}+\gamma_{\mathrm{a}}+\gamma_{\mathrm{p}})} \qquad \textbf{[4]}$$

Note that the noise strength can be thought of in integer units of molecules of protein. In our experimental setup, we measure noise strength in terms of arbitrary fluorescent units (AU); 1 AU corresponds to some unknown number of protein molecules. In Eq. 4, we have defined the average number of proteins produced per mRNA as the translational efficiency $E_{m\to p}$ (equal to k_p/γ_m), and the average number of mRNA produced per promoter activation event as the transcriptional efficiency $E_{a\to m}$ (equal to k_m/γ_a). This formulation eliminates the ratio between the means of various species, leaving behind the translational and transcriptional efficiency and obscuring the origin of each noise term. However, we can label each term relative to the original normalized variance terms in order to understand the source of the noise in protein levels:

$$\nu_{\text{int}} = \underbrace{1}_{\text{translation}} + \underbrace{E_{m\to p}\cdot\frac{\gamma_m}{\gamma_m+\gamma_p}}_{\text{transcription}} + \underbrace{E_{m\to p}E_{a\to m}\cdot\frac{(1-\langle a\rangle)(k_a+\gamma_a+\gamma_m+\gamma_p)\gamma_a\gamma_m}{(k_a+\gamma_a+\gamma_m)(\gamma_m+\gamma_p)(k_a+\gamma_a+\gamma_p)}}_{\text{gene activation}} \quad \textbf{[5]}$$

For example, the first term derives from translation. Our model contains the assumption that protein production from mRNA displays Poissonian statistics. If protein production in our model involved competition between the translation and degradation machinery, this first term would be larger than one, because translational events would occur with a geometric rather than Poissonian distribution, and the ratio of variance to mean of the geometric distribution is larger than one (*S19*). Alternatively, if translation were not a stochastic reaction, the first term would become zero. In such a case, the amount of noise strength would still change as translational efficiency changes. This can be understood intuitively by considering that when we multiplied all three terms of the normalized variance equation by protein mean to produce noise strength, we introduced a

dependence on protein mean to the gene activation and transcription components of the noise strength.

The noise strength equation can be simplified by assuming that protein degradation is infrequent compared to all other reactions in the model, and calculating the steady-state population mean of the active promoter in terms of the kinetic constants of promoter activation and deactivation:

$$\nu_{\text{int}} \approx \underbrace{1}_{\text{translation}} + \underbrace{E_{m\to p}}_{\text{transcription}} + \underbrace{E_{m\to p}\cdot\frac{k_m\gamma_a}{(k_a+\gamma_a)^2}}_{\text{gene activation}} \qquad \textbf{[6]}$$

This expression allows intuition of the three different cases detailed in the text and Fig. 3.

Case I

When both k_a and γ_a are similar in magnitude and much smaller than k_m, the third term is large relative to the other terms and is highly dependent on the k_a, and case I results. The noise strength in this case will decrease with an increasing rate of promoter activation, but will increase with increasing rate of transcription or translational efficiency. Intuitively, the effect of increasing the rate of promoter activation can be thought of as removing available substrate for the promoter activation step, which makes that promoter activation step behave in a less-than-Poissonian manner and causes the noise strength to decrease.

Case II

When k_a is much smaller than γ_a, and γ_a is approximately equal to or less than k_m, then the third term can be substantial relative to the other terms. The third term depends only on $E_{a\to m}$ and not on k_a, and case II results:

$$\nu_{\text{int}} \approx \underbrace{1}_{\text{translation}} + \underbrace{E_{m\to p}}_{\text{transcription}} + \underbrace{E_{m\to p}\cdot\frac{k_m}{\gamma_a}}_{\text{gene activation}} \quad \textbf{[7]}$$

The noise strength is not sensitive to changes in promoter activation but does scale with both the efficiency of transcription $E_{a\to m}$ and the efficiency of translation $E_{m\to p}$ (Fig. 3E).

Case III

When k_a and γ_a are both much larger than k_m, the third term, or contribution from the noise of gene activation, is very small and case III results:

$$\nu_{\text{int}} \approx \underbrace{1}_{\text{translation}} + \underbrace{E_{m\to p}}_{\text{transcription}} \quad \textbf{[8]}$$

The noise strength is not sensitive to changes in promoter activation or transcription, only to the efficiency of translation $E_{m\to p}$ (Fig. 3F).

A previously proposed model for noise generation in prokaryotes (*S18, S20*) suggested that the stochastic contribution of transcription to noise strength is modulated by the translational efficiency. In such a model, the actual stochasticity of translation contributes minimally to the variability in protein levels, but the measured noise strength scales with translational efficiency. This scaling factor led the authors to propose that, given a set of genes with equivalent stochasticity in transcription, those genes that are relatively inefficiently translated will be less phenotypically variable. Our model encompasses this possibility, and suggests additional situations where the stochasticity of transcription contributes little to population variability relative to the stochasticity of promoter activation. In these cases, the intrinsic noise strength of gene expression will scale with the efficiency of the transcriptional, as well as translational, step. This allows

direct selection of the noise in mRNA levels without modulation of translational efficiency.

Differentiating between case II and case III for *GAL1*

Both the *PHO84* and *GAL1* promoters display profiles that are consistent with either case II or case III of the model. If the *GAL1* promoter is an example of case III, the intrinsic noise strength has only transcriptional and translational contributions. The data from the TATA box variants of *PHO5* allow calculation of the maximal noise contribution from transcription and translation combined; this noise strength value is found at the limit as the k_m or transcriptional efficiency approaches zero (see the noise strength equation above). This value for *PHO5* is less than 0.25 AU, substantially smaller than the measured noise strength of the *GAL1* promoter of ~1 AU. If *GAL1* represents case III then *GAL1* must display a much higher noise strength from transcription than *PHO5*. The magnitude of the intrinsic noise strength contribution from transcription and translation is in theory dependent only on the translational efficiency of the reporter mRNA (Eq. 8). The *PHO5* and *GAL1* reporter mRNAs differ only in the 5' untranslated (5'UTR) region, and therefore in order for *GAL1* to fit the profile of case III, the 5'UTR of the *GAL1* reporter mRNA must confer a substantially higher translational efficiency than the 5'UTR of the *PHO5* reporter mRNA. Because the start sites of transcription have been identified for both *PHO5* and *GAL1* (*S21, S22*), we were able to replace the entire 5'UTR regions of the two promoters in order to test if the 5'UTR from *GAL1* conferred a substantial increase in both the rate of transcription and stochastic noise strength on the *PHO5* upstream promoter sequence, and vice versa. We found that

the promoters retain similar rates of induction and noise strength independent of 5'UTR identity (figure S5). Therefore we can hypothesize that the noise strength of *GAL1* does contain a substantial contribution from a promoter activation step prior to transcription, and corresponds to case II rather than case III. This assertion is consistent with the known role of chromatin-remodeling complexes in the activation of the *GAL1* promoter (*S23, S24*).

SUPPORTING FIGURES

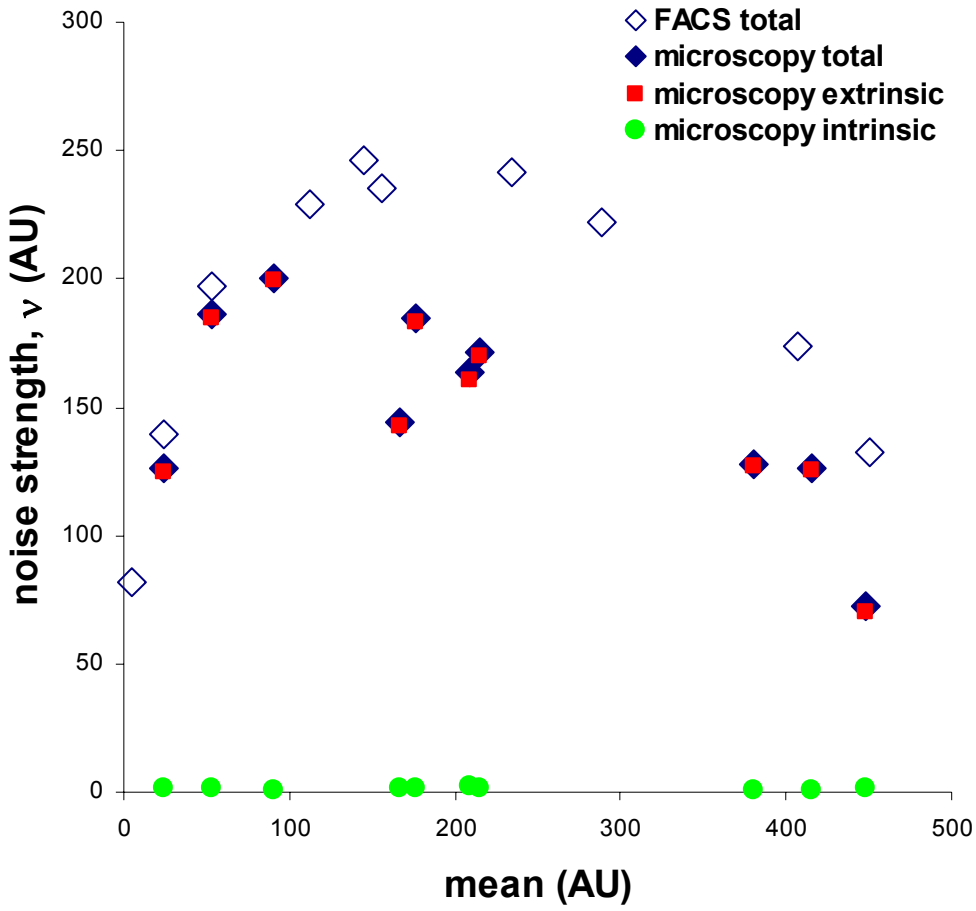

Fig. S1. Intrinsic, extrinsic, and total noise measurements for the yeast *GAL1* promoter. Noise strength of the *GAL1* promoter after eight hours of exposure to various levels of galactose. Noise strength was measured by flow cytometric quantification of YFP (◇), or dual-reporter microscopy and calculate of total (◆), intrinsic (●), and extrinsic (■) noise strengths. The flow cytometric measurements were scaled to microscopy arbitrary fluorescent units by maximal induction population mean.

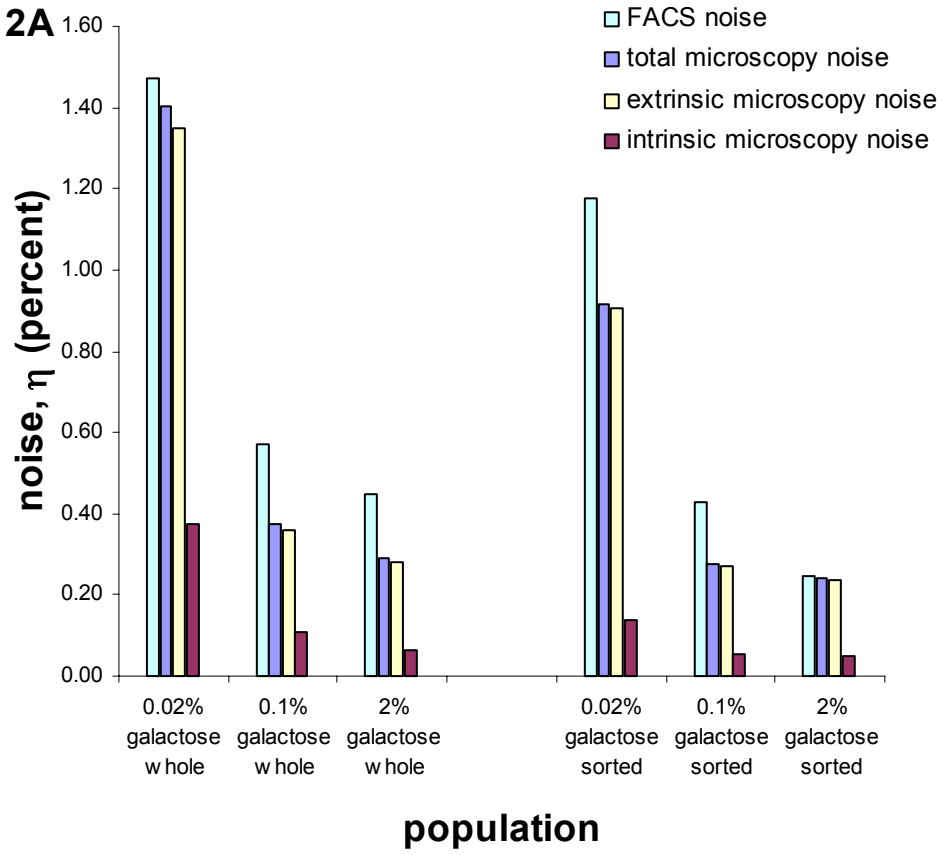
2A
FACS noise
total microscopy noise
extrinsic microscopy noise
intrinsic microscopy noise
noise, η (percent)
1.60
1.40
1.20
1.00
0.80
0.60
0.40
0.20
0.00
0.02% galactose whole
0.1% galactose whole
2% galactose whole
0.02% galactose sorted
0.1% galactose sorted
2% galactose sorted
population

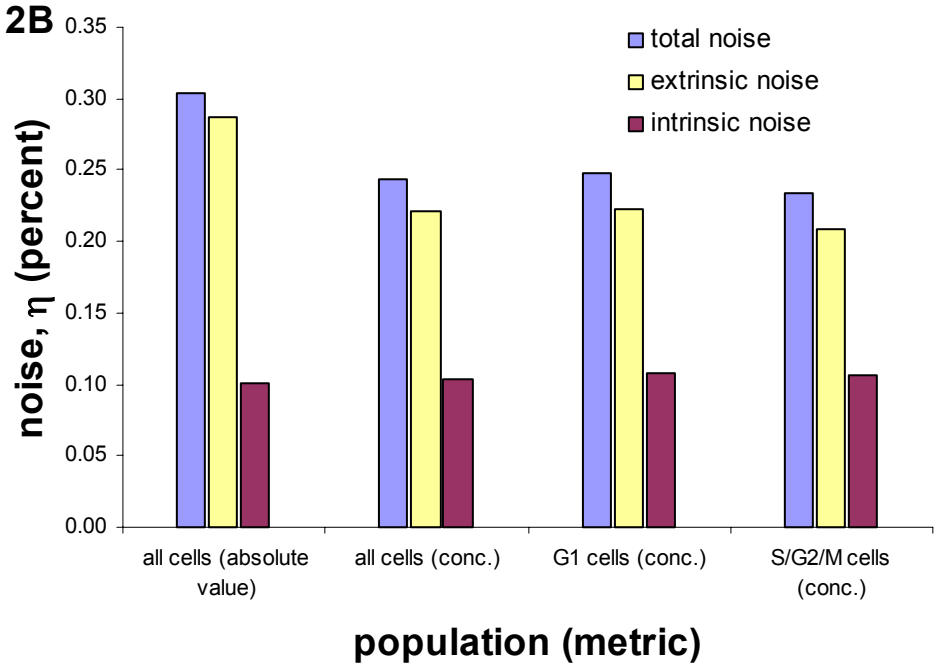
2B
total noise
extrinsic noise
intrinsic noise
noise, η (percent)
0.35
0.30
0.25
0.20
0.15
0.10
0.05
0.00
all cells (absolute value)
all cells (conc.)
G1 cells (conc.)
S/G2/M cells (conc.)
population (metric)

Fig. S2. Extrinsic noise reduction by cell shape, size, and cell cycle stage. (**A**) Total, intrinsic, and extrinsic noise of *GAL1*-expressing populations before ("whole") and after sorting ("sorted") by flow cytometry cell size criteria (forward-scatter and side-scatter gating). The *GAL1* promoter was induced by the indicated concentrations of galactose for one hour prior to measurement. (**B**) Total, intrinsic, and extrinsic noise of *PHO5*-expressing populations before ("absolute value") and after correction for variation in cellular volume ("conc."), and in populations stratified by cell cycle stage after correction for cellular volume.

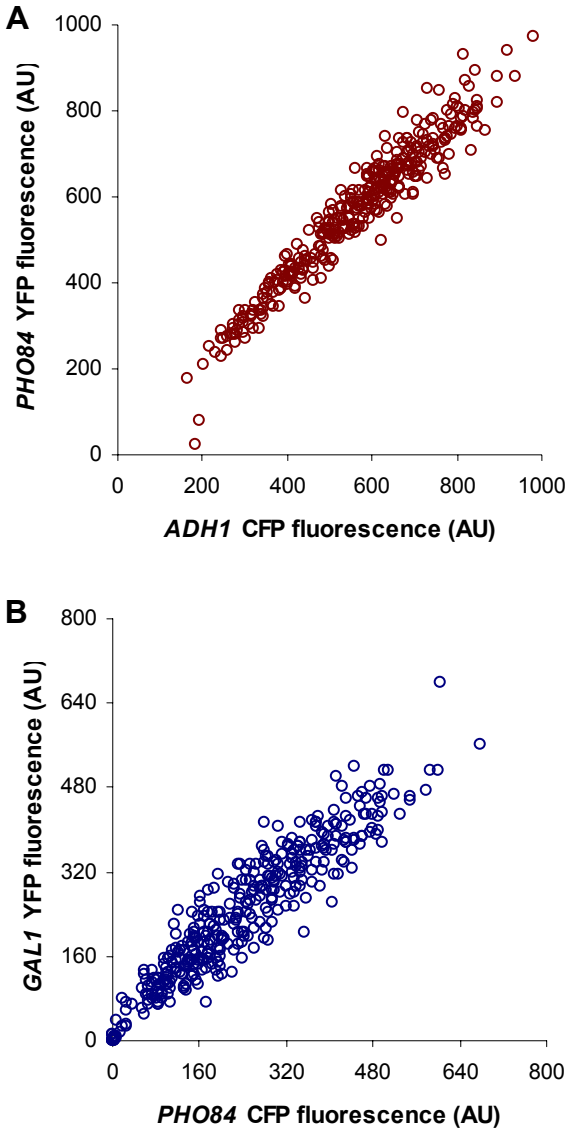

Fig. S3. Correlated expression from two different promoters. (**A**) Scatter plot of cells expressing YFP from the *PHO84* promoter and CFP from the *ADH1* promoter. $R^2 = 0.93$; *PHO84* noise is 30% and *ADH1* noise is 30%. (**B**) Scatter plot of cells expressing YFP from the *GAL1* promoter and CFP from the *PHO84* promoter. $R^2 = 0.88$; *PHO84* noise is 58% and *GAL1* noise is 53%. For each scatter plot, cells from three separate measurements are shown.

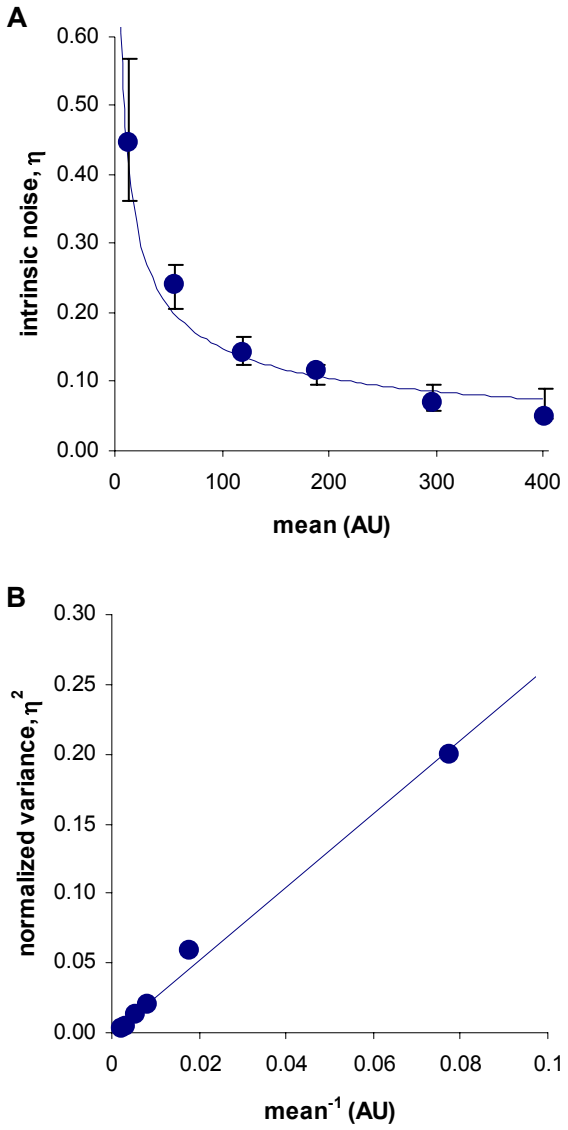

Fig. S4. Intrinsic noise is consistent with a stochastic process. (**A**) Intrinsic noise as a function of population mean for populations from the *PHO5* induction time course shown in Fig. 1B. Error bars are calculated by the bootstrap method (see materials and methods section). (**B**) Intrinsic normalized variance as a function of the inverse mean for the same data. For both plots, the solid lines represent expectations for a single underlying stochastic process.

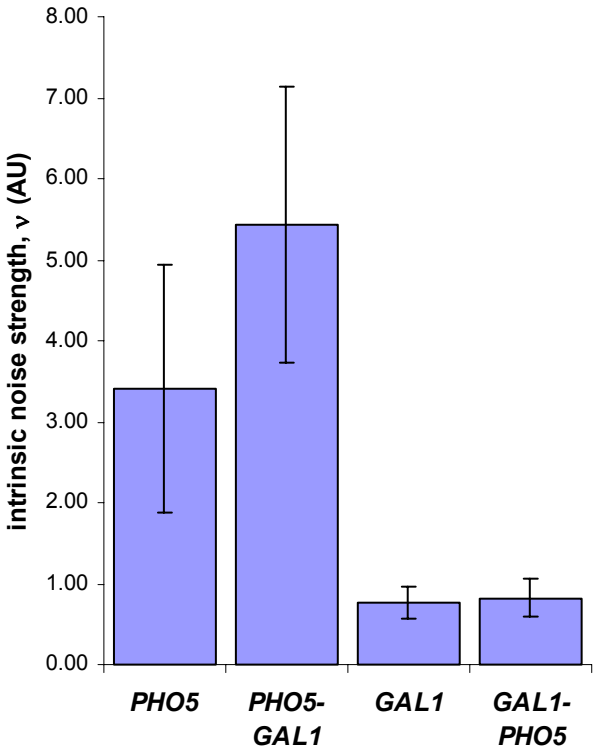

rate of expression:	100%	104%	100%	72%

Fig. S5. Exchange of 5' untranslated regions of *GAL1* and *PHO5* promoters. Intrinsic noise strength was measured for the *PHO5* and *GAL1* promoters and for fusion promoters containing the *PHO5* upstream sequences and *GAL1* transcription start site region (*PHO5-GAL1*), or the *GAL1* upstream sequence followed by the *PHO5* transcription start site region (*GAL1-PHO5*). The rates of gene expression as a percentage of the rates of the wild-type *PHO5* and *GAL1* promoters are shown below the graph.

SUPPORTING MATERIAL REFERENCES

S1. B. P. Cormack *et al.*, *Microbiology* **143 (Pt 2)**, 303 (1997).
S2. A. Crameri, E. A. Whitehorn, E. Tate, W. P. Stemmer, *Nat Biotechnol* **14**, 315 (1996).
S3. R. Heim, R. Y. Tsien, *Curr Biol* **6**, 178 (1996).
S4. K. R. Siemering, R. Golbik, R. Sever, J. Haseloff, *Curr Biol* **6**, 1653 (1996).
S5. O. Griesbeck, G. S. Baird, R. E. Campbell, D. A. Zacharias, R. Y. Tsien, *J Biol Chem* **276**, 29188 (2001).
S6. T. Nagai *et al.*, *Nat Biotechnol* **20**, 87 (2002).
S7. E. Alani, L. Cao, N. Kleckner, *Genetics* **116**, 541 (1987).
S8. H. Miyasaka, *Yeast* **15**, 633 (1999).
S9. D. J. Steger, E. S. Haswell, A. L. Miller, S. R. Wente, E. K. O'Shea, *Science* **299**, 114 (2003).
S10. M. Springer, D. D. Wykoff, N. Miller, E. K. O'Shea, *PLoS Biol* **1**, E28 (2003).
S11. A. S. Carroll, A. C. Bishop, J. L. DeRisi, K. M. Shokat, E. K. O'Shea, *Proc Natl Acad Sci U S A* **98**, 12578 (2001).
S12. M. A. Gibson, J. Bruck, *Journal of Physical Chemistry A* **104**, 1876 (2000).
S13. D. T. Gillespie, *J. Phys. Chem.* **81**, 2340 (1977).
S14. P. S. Swain, M. B. Elowitz, E. D. Siggia, *Proc Natl Acad Sci U S A* **99**, 12795 (2002).
S15. J. Paulsson, *Nature* **427**, 415 (2004).
S16. M. B. Elowitz, A. J. Levine, E. D. Siggia, P. S. Swain, *Science* **297**, 1183 (2002).
S17. W. J. Blake, M. Kaern, C. R. Cantor, J. J. Collins, *Nature* **422**, 633 (2003).
S18. M. Thattai, A. van Oudenaarden, *Proc Natl Acad Sci U S A* **98**, 8614 (2001).
S19. H. H. McAdams, A. Arkin, *Proc Natl Acad Sci U S A* **94**, 814 (1997).
S20. E. M. Ozbudak, M. Thattai, I. Kurtser, A. D. Grossman, A. van Oudenaarden, *Nat Genet* **31**, 69 (2002).
S21. J. Svaren, W. Horz, *Trends Biochem Sci* **22**, 93 (1997).
S22. C. Giardina, J. T. Lis, *Science* **261**, 759 (1993).
S23. E. Larschan, F. Winston, *Genes Dev* **15**, 1946 (2001).
S24. M. S. Santisteban, T. Kalashnikova, M. M. Smith, *Cell* **103**, 411 (2000).